23rd ABCM International Congress of Mechanical Engineering
December 6-11, 2015, Rio de Janeiro, RJ, Brazil

DEVELOPMENT OF AN AXIAL - TORSION BIAXIAL FATIGUE TESTING MACHINE

Eleazar Cristian Mejia Sanchez
Marco Antonio Meggiolaro
Jaime Tupiassú Pinho de Castro
Pontificia Universidade Catolica do Rio de Janeiro, PUC-Rio
crisms@tecgraf.puc-rio.br
meggi@puc-rio.br
jtcastro@puc-rio.br

Abstract. *The experimental evaluation of incremental plasticity models and multiaxial fatigue life prediction require the use of multiaxial testing machines. In this paper, an axial-torsion biaxial machine is developed and applied to perform multiaxial fatigue tests. This innovative electromechanical system uses two DC motors connected to gearboxes to generate axial and/or torsion loads. The design of the axial-torsion machine comprises the analysis of its structural integrity, component dimensioning and fatigue life prediction, complete modeling of the resulting dynamic system, development of a control technique, and finally its construction and testing. The control technique applied is a PID sliding control, which combines the advantages of a PID and sliding control. The optimal values of control parameters (proportional, integral, derivative) allow reaching the desired control response and avoid overshoot. The proposed sliding mode controller is chosen to ensure the stability of this electromechanical system. The controller is able to independently specify the axial force and torque load to be applied, being implemented in LabVIEW software running in a cRIO-NI control system. The inputs for both control systems are the error values of each load to be applied to the test specimen. The tension-torsion machine is designed to meet the requirements of a wide range of multiaxial fatigue tests, with a maximum axial force capacity of ±200kN and ±1300N.m torque capacity. The performance of the electromechanical system is experimentally evaluated from stress-strain multiaxial test results.*

Keywords: *PID Sliding Control, Electromechanical Test Machine, Axial-Torsion Test Machine, Multiaxial Fatigue*

1. INTRODUCTION

In general, traditional fatigue testing machines are developed using servo-hydraulic systems and they are focused to predict the useful life service of materials in uniaxial testing. The multiaxial machines are very expensive because they require two or more actuators, and a very rigid structure. The acquisition of these machines are infeasible for educational purposes. The real loads of service frequently actuate in different points of the piece, and which may come from one and multiples fonts. Real loads induce axial force, torsion, bending, normal or shear stress. The combination of these stresses could generate bi or tri variable stresses at the critical point of piece. The fatigue process in these situations is known as multiaxial fatigue (Meggiolaro and Castro, 2009). The critical point of many mechanical components undergoes multiaxial cyclic loads during its useful life. The problem of multiaxial fatigue is more complex because both, the stress distribution and crack initiation, have different directions within the component (Yongming and Sankaran, 2005). The multiaxial fatigue-testing machine developed by Instron Company are based on servo-hydraulic system actuators, with tensile/compression capacity in the range of 2 kN until 250 kN and torsion in the range of 100 N.m until 2000 N.m (Instron, 2012). These machines use a PID control and their parameters are optimized during the test according to the changes of the characteristics in the specimen test (ST). In the last two decades, biaxial testing machine are used to study incremental plasticity, where the ST is subjected to a complex multiaxial loading to obtain cyclic strain path. The study made by Takamoto shows the experimental evaluation of a simple two-surface model for incremental plasticity based on kinematic hardening rule under non-proportional loading of stainless steel 304 (Takamoto I, 1999). In order to study incremental plasticity models, this paper presents the design and development of an axial-torsion machine (ATM) with electric actuators. The work includes the structural analysis, modeling of control system and load/torsion transducers. Finally, the developed biaxial machine is used for experimental evaluation of incremental plasticity models. All experiments are conducted in fatigue laboratory at PUC-Rio.

2. DESIGN AND MODELLING OF AN AXIAL TORSION MACHINE

The ATM structural integrity includes the following topics: First, a general description of this machine; Secondly, a determination of the maximum force and moment required and finally, a study of its axial and torsion stiffness.

2.1 Determination of axial load and torsion

The ATM was designed to work with a maximum capacity of ± 200 kN in tensile, while the maximum torsional moment, required by the machine to produce the same effect on the ST in pure tensile as pure torsion was computed based on the maximum shear stress criterion. A tubular test specimen (TST) of thin-walled was chosen to compute the torsion moment T, the stress profile due to torsion on the tubular specimen can be considered always constant.

The maximum tensile on the TST generates a yield stress S_E and shear stress τ_E, according to the maximum shear stress criterion, the system may generate the same effect under tensile and torsion. Then, the maximum torsional moment to generate the same shear stress is given by,

$$T = \frac{S_E . J}{2\rho} \tag{1}$$

where, T is the torsional moment in pure torsion, J is the polar inertial moment and ρ is the average radius of TST. Then, the maximum torsional moment T for a TST of stainless steel was obtained replacing the values of D_e = 25 mm , D_i = 20 mm, and S_E=1400 MPa in equation 1.

$$T = \frac{\pi . S_E . (D_e^2 - D_i^2)}{32 . D_e} = 1278 \text{ N.m} \tag{2}$$

Therefore, the Axial-Torsion Machine was designed to generate P = ±20 kN maximum axial force and T = ±1300 N.m of maximum torsional moment.

2.2 Axial stiffness of ATM

The axial stiffness is the ability to resist attempts of stretching or shortening due the application of load. The axial displacement generated by the maximum axial force P=250 kN was calculated using the Ansys software.

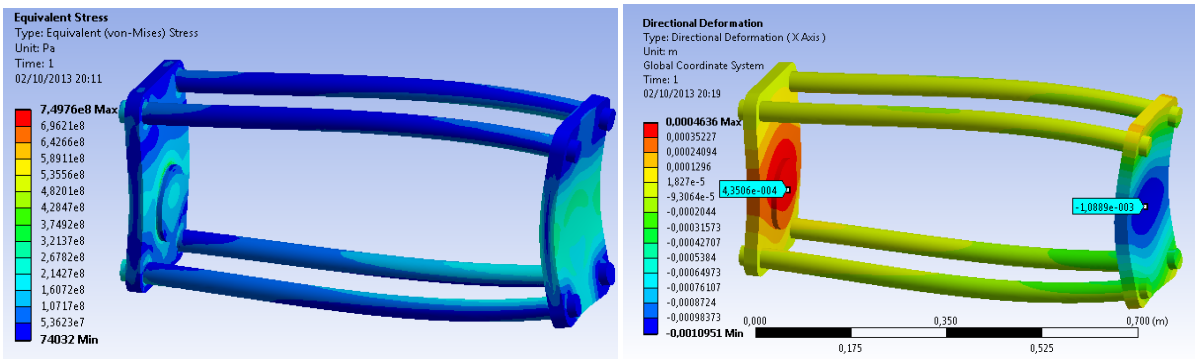

a) b)

Figure 1. a) Stress and b) displacement in direction "x" of reduced model of ATM

The total displacement is given by the subtraction of right side δ_D = -0,0010889 and left side δ_I = 0,000435 then $\delta_{Total} = |\delta_D - \delta_I| = 0{,}0015239$ as shown in figure 1.b. A reduced model was used to calculate the axial stiffness of the ATM, $K_P = 250000/(15{,}2396\ 10^{-4})$, then K_a = 164 MN/m. The buckling strength P ≅ 100 MN in pure tensile was evaluated using Ansys software due to the ATM had thin columns and it was subjected to high loading.

2.3 Rotation stiffness of ATM

The rotation stiffness is defined as the ability to resist rotation as a result of the application of torsional moment and it is calculated as $K_T = T/\alpha$. The rotation angle α generated by the torsional moment T can be calculated by the following equation $\alpha = 2.\arcsin(\delta_z / L)$, where δz is the displacement in "z" and L is the beam length as shown in figure 2. The rotational angle $\alpha = 0{,}002$ rad was calculated for the applied torsional moment T = 1300 N.m. Therefore, the calculated rotation stiffness of ATM is $K_T = 1300/0{,}002 = 650$ kN.m/rad. Finally, the maximum torsional moment T ≅ 645 kN.m that generate buckling problems in pure torsion was evaluated.

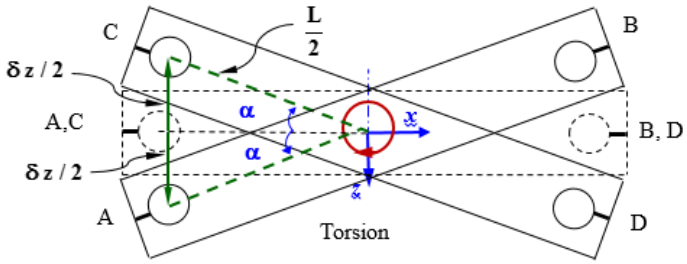

a) b)

Figure 2. Rotation of AB and CD beam subjected to torsional moment

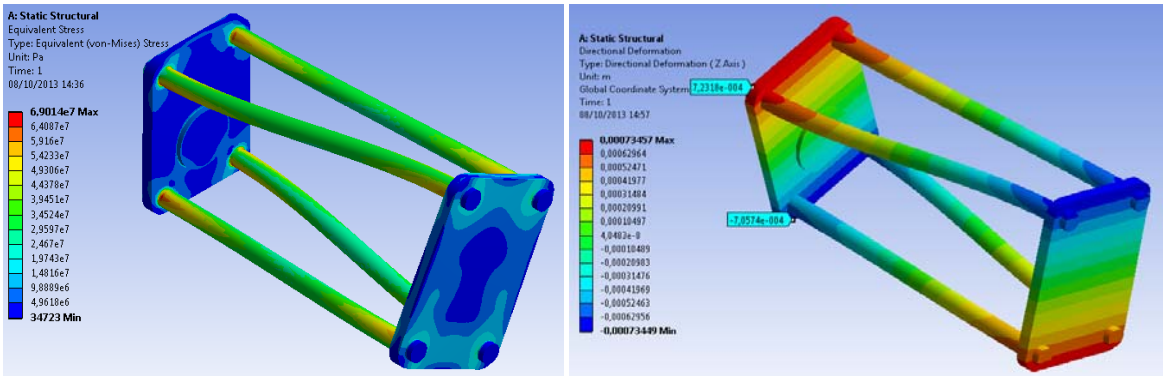

a) b)

Figure 3. a) Stress and b) displacement in direction "z" of reduced model of ATM

2.4 Development of load torque cell

For the proper operation of ATM is necessary to have a transducers that it is used to measure the level of axial force and torsional moment applied over ST. In the industry, this equipment is very expensive; then, a load torque cell (LTC) transducer was designed and developed to measure the loads applied by the ATM over ST. The LTC was designed to measure the traction/compression and torsion loads or combination of them, as show in figure 4.

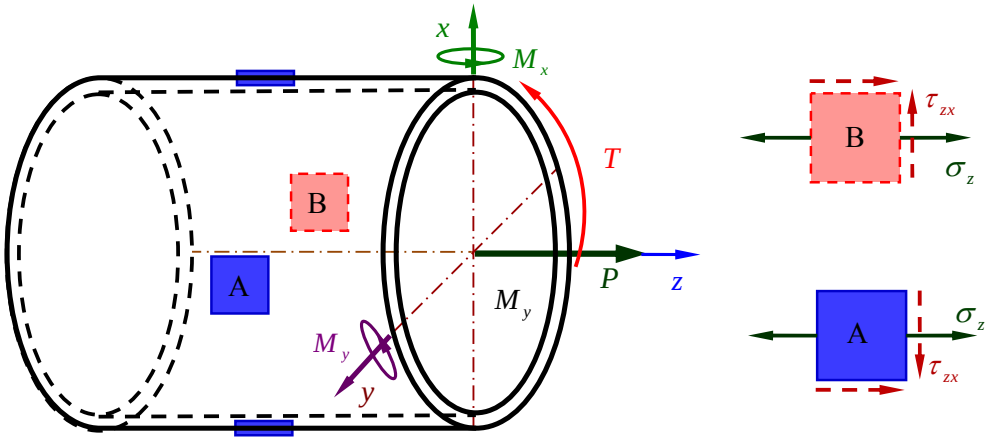

Figure 4. Hollow circular section at the middle of LTC structure

In figure 4 shows the shape of critical section of LTC structure, it is a hollow circular section located in the transducer center. The normal σ_z and shear τ_{zx} stress are generated by the axial load P and torsional moment T. In figure 5.a, the points A and B are subjected an normal stress $\bar{\sigma}_A^P = \bar{\sigma}_B^P = (\sigma_z \ 0 \ 0 \ 0 \ 0 \ 0)^T$ generated by the axial load P, On the other hand, in figure 5.b, these points are subjected shear stress $\bar{\sigma}_A^T = \bar{\sigma}_B^T = (0 \ 0 \ 0 \ \tau_{zx} \ 0 \ 0)^T$ generated by the torsional moment T. The LTC was designed to work in the elastic zone, therefore, strains are calculated using the Hooke's law $\bar{\varepsilon} = \bar{E}^{-1}.\bar{\sigma}$, where, $\bar{\varepsilon}$ is the strain tensor and $\bar{E}^{-1}$ is Hooke's elastic compliance matrix.

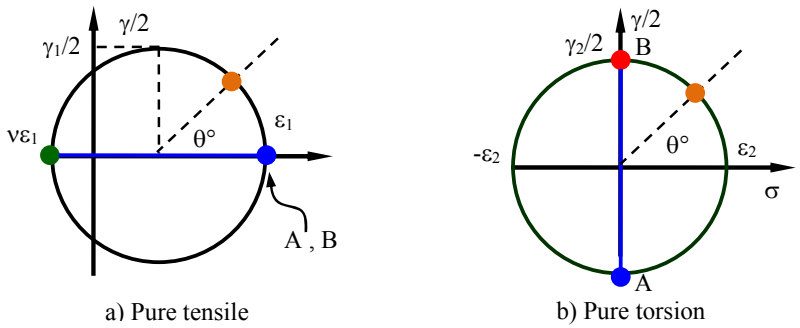

a) Pure tensile b) Pure torsion

Figure 5. Typical deformation state through of the Mohr circle

In Figure 5, the strains ε_1, ε_2, γ_1 and γ_2 are given by the following expression, $\varepsilon_1 = E^{-1}.\sigma_z$ and $\gamma_{zx} = \tau_{zx}/(2G)$, where E is the elasticity modulus and $G = E/[2.(1+\nu)]$ is the shear modulus. In the case of pure tensile, the strains at the points A and B for 0°, 45° and 90° angle are given by $\varepsilon^P_{0°} = \varepsilon_1$, $\varepsilon^P_{45°} = \varepsilon_1.(1-\nu)/2$ and $\varepsilon^P_{90°} = -\nu.\varepsilon_1$, while in pure torsion, these strains are given by $\varepsilon^T_{0°} = \varepsilon_2$, $\varepsilon^T_{45°} = 0$ and $\varepsilon^T_{90°} = -\varepsilon_2$. Finally, the total strains are calculated using the superposition principle as $\varepsilon^{total}_{0°} = \varepsilon^P_{0°} + \varepsilon^T_{0°} = \varepsilon_1 + \varepsilon_2$, $\varepsilon^{total}_{45°} = \varepsilon^P_{45°} + \varepsilon^T_{45°} = \varepsilon_1(1-\nu)/2$ and $\varepsilon^{total}_{90°} = \varepsilon^P_{90°} + \varepsilon^T_{90°} = -(\nu.\varepsilon_1 + \varepsilon_2)$. Where $\varepsilon^P_{\theta°}$, $\varepsilon^T_{\theta°}$ and $\varepsilon^{total}_{\theta°}$ are the strain at $\theta°$ in relation of "z" axis due the axial force P, torsion moment T and combination of both load, respectively.

Table 1. Material Properties of the LTC.

Material properties	**4340 steel**
Elasticity modulus E (GPa)	210
Shear modulus G (GPa)	80,7
Poisson constant **ν**	0,3
Maximum axial load P (kN)	200
Maximum torsional Moment T (N.m)	1300

The normal stress σ_z = 196 MPa and shear stress τ_{zx} = 42 MPa at the center of LTC structure are generated by the axial force and torsion moment applied. The strains in pure tensile $\varepsilon^P_{0°} = 933\ \mu\varepsilon$, $\varepsilon^P_{45°} = 326\ \mu\varepsilon$, $\varepsilon^P_{90°} = -280\ \mu\varepsilon$ and in pure torsion $\varepsilon^T_{0°} = 260\ \mu\varepsilon$, $\varepsilon^T_{45°} = 0\ \mu\varepsilon$, $\varepsilon^T_{90°} = -260\ \mu\varepsilon$ were calculated using the Hooke's law. Then, the total strains measured by the strain gage are: $\varepsilon^{total}_{0°} = 1192\ \mu\varepsilon$, $\varepsilon^{total}_{45°} = 326\ \mu\varepsilon$, $\varepsilon^{total}_{90°} = -540\ \mu\varepsilon$. The maximum strain $\varepsilon^{total}_{0°} = 1192\ \mu\varepsilon$ is located at the center of LTC structure due to the combination of axial force and torsional moment. According to the technical specification of Micro-Measurement Vishay Company (Hannah and Reed, 1992), the strain-gage used at LTC have a 100 million cycles of fatigue life for total strain $\boldsymbol{\varepsilon < 1500\ \mu\varepsilon}$. The LTC was designed to support the maximum axial and torsional loading as show in Figure 6.a.

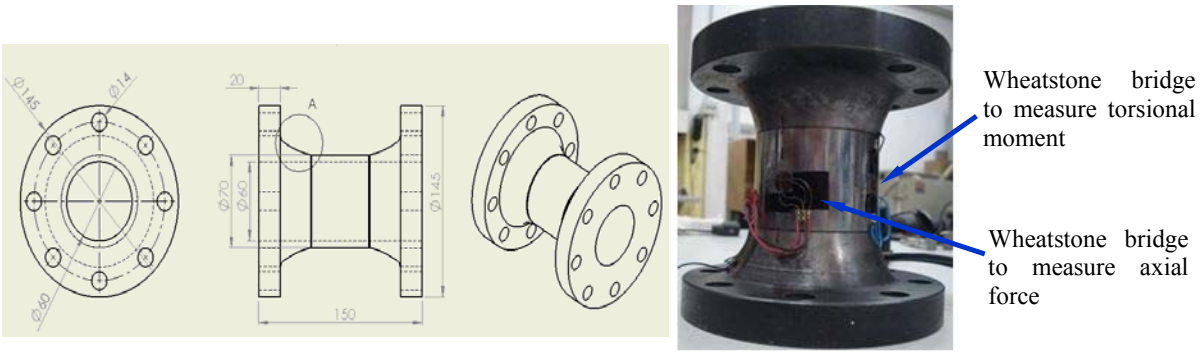

Figure 6. LTC design a) General scheme b) developed Load torque cell at PUC-Rio's Laboratory of fatigue.

The shape of LTC notches was optimized to minimize the stress concentration factor to increase the fatigue life. This optimization consists in the addition or removal material to change the notches' shape according to the value of stress concentration factor (Alburquerque, 2012). The strain gages are bonded at the center of LTC structure and they are connected in two full Wheatstone bridge circuits. The first bridge is used to measure axial force and the second one is used to measure torsion moment. The strain gauge configuration at the four arms of Wheatstone bridge allows the strain compensation and it is generated by eccentric load, the effect of temperature and strain due to the torsional moment in axial load measurement and reciprocally. The alloy steel 4340 was used in the LTC construction because of its well-established heat-treating practices and easy to machine (Hannah and Reed, 1992). The LTC was machined in ROMI - CENTUR 3D universal CNC lathe and it was submitted to heat treatment (to get a hardness of 48 RHC). The figure 6.b shows the LTC developed at PUC-Rios's fatigue laboratory.

2.5 Design of an axial torsion machine

The ATM is composed for load transmission elements, two mechanical actuators, transducers for measurement of the variable to be controlled, a control system provided with user-machine interface and the mechanical structure as shown in figure 7. This electromechanical system created for multiaxial fatigue testing consists of an arrangement of individual and interconnected components to provide traction and/or torsion on the ST. The ATM was designed to work with a maximum capacity of 25 kN in traction and 1300 N.m in torsion, which is able to produce the same effects on the ST in pure tensile or pure torsion. The designed axial-torsion machine is shown in figure 7.

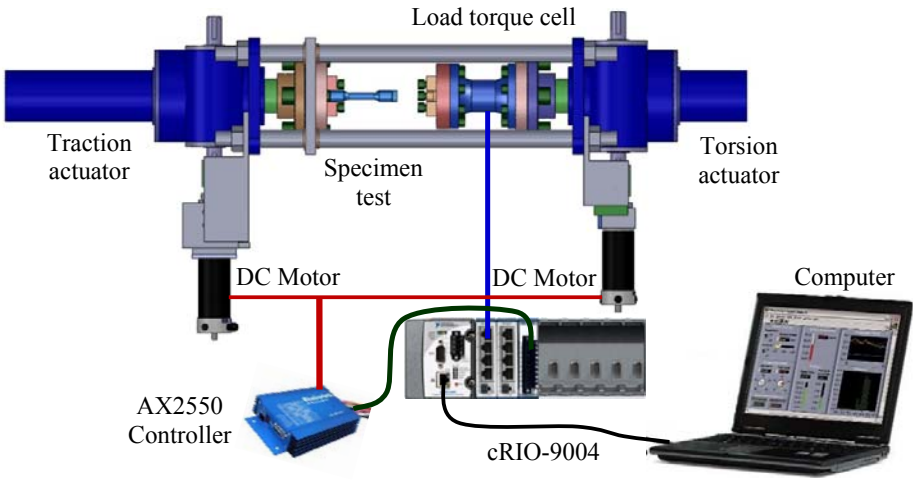

Figure 7. General scheme of ATM designed

3. CONTROL SYSTEM OF ATM

The axial force and torsional moment applied by the ATM on the ST is controlled independently to experimentally assess of incremental plasticity models. The main challenge to design the ATM controller was to overcome the nonlinearities in the ATM, such as, friction in the columns, dead-zone, saturation and backslash in the actuators and gear motor. The controller based on sliding mode technique was implemented to overcome the nonlinearities of the ATM.

3.1 Design of axial force controller

The axial force applied on the ST is the measured process variable used to design the force control. Thus, the error value e_F is calculated as the difference between a measured axial force $x = F_r$ and desired force $x_d = F_d$. Then, the force controller output u_F is given by the following equation,

$$u_F = k_{sF} \,.\, \text{sat}(S_F) \tag{3}$$

where, k_{sF} is the switching gain, sat() is the saturation function and S_F is the sliding surface. The sliding surface is calculated as $S_F = \dot{e}_F + \lambda . e_F$, where λ is the proportional gain, e_F and $\dot{e}_F$ are the error and derivative error, respectively (Slotine, 1991) (Liu and Wang, 2012) (Perruqueti and Barbot, 202).

3.2 Design of the torsional controller

The control of torsional moment requires the design of a more robust controller due to its high sensibility of load torque cell. The ATM generates a high measurement of the torsional moment for small angular displacements of the torsional actuator. The hybrid controller was implemented to overcome the challenges of torsional controller. This control is called as PID sliding control and it combines the advantages of PID and sliding control. In this hybrid control, the sliding surface is calculated as the output of a PID controller, in function of the measured error value (e).

Then, the error value e_T is calculated as the difference between the measured torsional moment $x = T_r$ and the desired torsional moment $x_d = T_d$ as $e_T = T_r - T_d$. The output of torsional moment controller u_F is given by,

$$u_T = k_{sT} \cdot \text{sat}(S_T) \tag{4}$$

where, k_{sT} is the switching gain, sat( ) is the saturation function and S_T is the sliding surface. The sliding surface is calculated as $S_T = \dot{e}_T + \lambda_1 . e_T + \lambda_2 . \int e_T . dt$, where λ_1, $\lambda_2 > 0$ are the proportional and integral gain, respectively, e_T and $\dot{e}_T$ are the error and derivative error, respectively (Fallahi and Azadi, 2009). The general scheme of ATM control system is constituted by two-feedback loop as shown in the follow block diagram.

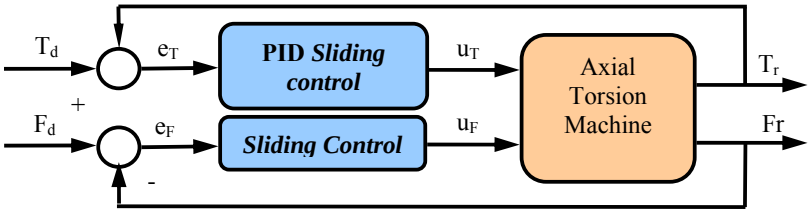

Figure 8. Scheme of the ATM modeling

4. EXPERIMENTAL SYSTEM AND RESULTS

The ATM developed at PUC-Rio's Laboratory of Fatigue is composed for two mechanical actuators, load transmission elements, transducers to measurement of the variable to be controlled, a control system provided with user-machine interface and the mechanical structure as shown in figure 9. The electric connections of ATM are constituted by two parts. First, the data reading that includes the connection of load torque cell and LVDT's to NI-9237 data acquisition module of the CompactRio, this module is provided by National Instrument; and second, The control system connection that includes the connection of cRIO NI-9263 to AX2550 controller, which controls the DC motor with a proportional control.

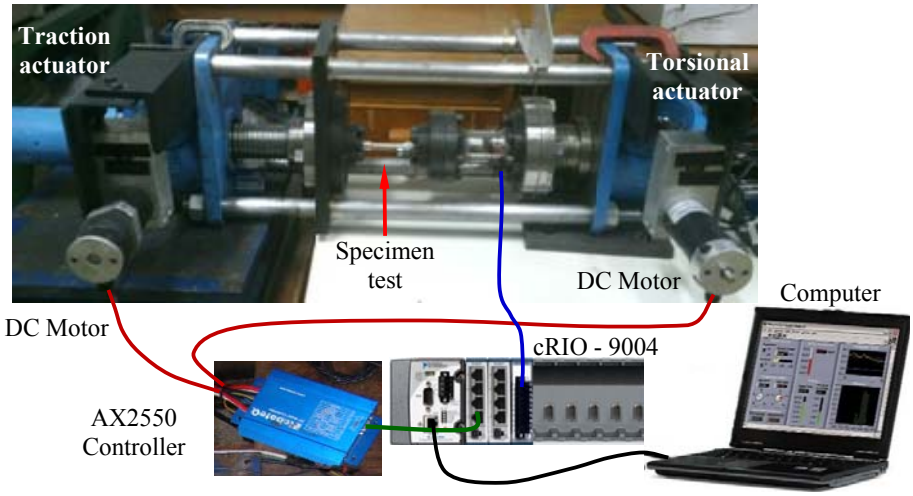

Figure 9. ATM developed at PUC-Rio's laboratory of Fatigue

The control system of ATM was developed using the compactRIO CRio-9004. It was developed using LabVIEW 9.0 to perform the tests on the experimental system described above, which includes acting on the system and reading data. The user can visualize the errors in real time, paths of the desired loads, paths of axial force and torque, paths of normal and shear stress, as well as position and rotation values. The ATM was used for experimental evaluation of an incremental plasticity model experimentally.

4.1 Experimental results

The ATM is used for experimental evaluation of a non-proportional (NP) hardening model. This incremental plasticity testing consists in subjecting the ST to a desired traction $\sigma(t) = \sigma_a.\sin(\omega t)$ and a desired torsion 90° out-of-phase $\tau(t) = \tau_a.\cos(\omega t)$ in load and torque control, respectively, where $\tau_a = \sigma_a.\sqrt{3}$. Figure 10 shows the experimental results for a desired load $\sigma_a = \pm$ 50 kN and desired torque 90° out-of-phase $\tau_a = \pm$ 189 N.m in load and torque control, respectively.

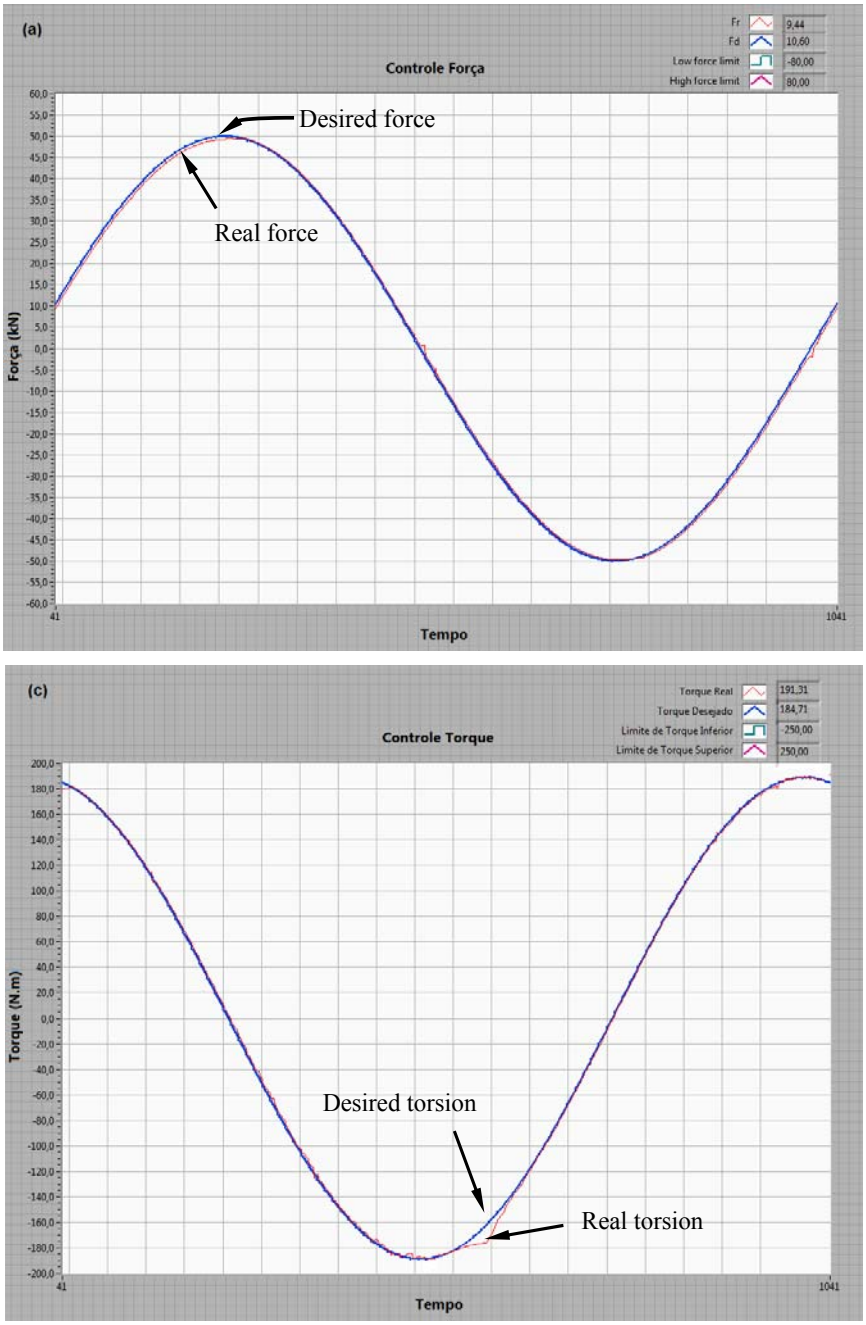

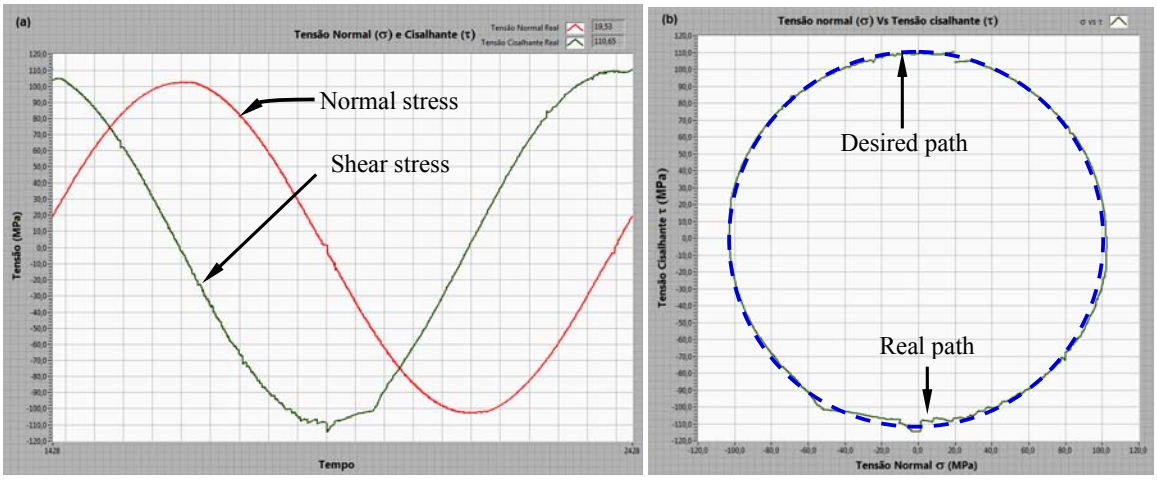

Figure 10. a) Load control b) Torque control c) Normal and shear stress d) plot σ_x vs $\tau_{xy}\sqrt{3}$

5. CONCLUSIONS

In this work, an ATM was developed at low cost for multiaxial fatigue testing. This machine has an axial force in the range of ±200 kN and torque capacity of ±1300 N.m. which allows a wide range of multiaxial fatigue tests. The design of the load toque cell involved the measurement of the axial force and torsion moment generated by the ATM. The strain gage configuration in the Wheatstone bridge of force and torque consider the compensation of eccentric loads, temperature effects, and torsion influence in the traction measurements and vice-versa. The PID sliding control overcame the nonlinearities in the ATM system.

The development of an axial - torsion machine is very important for the Laboratory of fatigue at PUC-Rio due to this machine will allow the experimental evaluation the plasticity incremental models.

6. REFERENCES

Albuquerque, D., 2012. "On the improved and the optimum notch shape", Pontificia Universidade Catolica de Rio de Janeiro, 56 pp.

Fallahi, M.; Azadi, S., 2009. Robust control of DC motor using fuzzy sliding control with PID compensator, Poceedings of the international multiconference of engineers and computer scientists, Vol II, Hong Kong.

Hannah, R.L.; Reed, S.E., 1992. "Strain Gage User's Handbook", London, Elseiver, 294 pp.

Instron Brasil, Al. Tocantins 280 - Unidade 7 Alphaville Industrial 06455-020 - Barueri, SP, Brasil.*http://www.instron.com.br/wa/product/MultiAxial-Test-Systems.aspx.*

Liu, J.; Wang, X., 2012. "Advanced sliding mode control for mechanical systems - Design, Analysis and MATLAB simulation", Springer, New York.

Meggiolaro, M.A., Castro, J.T.P, 2009. Tecnicas practicas de Dimensionamiento estrutural sobre reais em serviço – Vol I, Rio de Janeiro, CreateSpace, pp. 423-426.

Micro-Measurements, 2011. "Transducer Class Strain Gage" Vishay Precision Group. USA.

Perruquetti, W.; Barbot, J.P., 2002. Sliding mode control in enginnering, CRC Press.

Slotine, J. J.; Li, W., 1991. Applied nonlinear control, Prentice Hall, New jersey, 1991.

Takamoto, I.; Nakata, T.; Nasakane, M., 1999. “non-proportional low cycle fatigue of 6061 aluminum alloy under 14 strain paths, European strucutral integrity society, vol. 25, pp. 41-54.

Yongming. L., Sankaran, M.,2005. “Multiaxial High-Cycle Fatigue Criterion and Life Prediction for Metals”. Department of Civil and Environmental Engineering, USA.

7. RESPONSIBILITY NOTICE

The authors are the only responsible for the printed material included in this paper.